13th International Symposium on Particle Image Velocimetry – ISPIV 2019
Munich, Germany, July 22-24, 2019

Time-resolved Stereo-PIV measurements of complex flows in automotive headlamp

Mirae Kim[1], Dong Kim[1], Eunseop Yeom[1], and Kyung Chun Kim[1]*

[1]Pusan National University, School of Mechanical Engineering, Busan 46241, Korea

*kckim@pusan.ac.kr

Abstract

Automotive headlamps undergo environmental changes such as radiation from outside and heat from the engine. Thus, the internal flow characteristics have an unsteady flow regime due to heat transfer depending on the lighting state of the internal bulb. In this study, we measured the quantitative 2D3C velocity vector field in a headlamp with a complex shape using stereoscopic particle image velocimetry (SPIV) to determine the area that is vulnerable to condensation. In order to obtain the 3D velocity component and calibration for the image distortion, the calibration function was obtained using a calibration target. An olive oil aerosol was used as PIV-tracking particles. The particles were injected by a Laskin nozzle through the bent hole of a headlamp model. The SPIV measurements showed that the flow inside the headlamp has a strong 3D velocity component. It was found that two or more vortex components formed in a direction perpendicular to the main flow based on the natural convection. The Reynolds stresses were analyzed using a statistical method based on the instantaneous velocity components, and most of the flow fields had laminar flow characteristics. However, in the case of a bulb-type headlamp, turbulence was locally generated due to a thermal plume induced by the high temperature from the bulb surface and complex internal structures in the headlamp, such as the reflector.

1 Introduction

Weight reduction and energy savings for automotive headlamps have become important. The lens material conventionally used was glass, and metal was used for the reflectors, but they have been changed to plastic materials. The light source is also being converted from halogen lamps to LEDs. As a result, the space inside headlamps has become very complex. There are problems with thermal deformation of the material and condensation on the lens surface. The condensation is due to moist air and the temperature difference between inside and outside of the headlamp. In order to solve these problems, it is necessary to provide an accurate thermal flow analysis in the design stage.

Generally, there are three mechanisms for the inflow of moist air into a headlamp: the permeation of external moisture through the plastic directly into the headlamp, water coming out from the plastic itself due to the temperature rise from sunlight, and water inflow through a vent system for pressure balance. From these mechanisms, the moist air increases the absolute humidity in the headlamp. Condensation is generated on the inner surface of the lens if environmental conditions occur where the external temperature becomes lower than the internal temperature of the headlamp due to rain or a large temperature difference.

As computational fluid dynamics (CFD) analysis and computer performance have developed, it has become possible to predict the complex thermal and fluid phenomena inside an automotive headlamp. However, there is not enough assurance of the CFD results due to a lack of experimental data to verify them. Because of the complex shape of the headlamp, it is very difficult for an experimental approach

to quantitatively measure the flow using methods such as particle image velocimetry (PIV) and laser Doppler velocimetry (LDV). Therefore, only a few researchers have studied quantitative flow measurements inside a headlamp.

To the best of our knowledge, a few attempts have been made to measure the velocity fields inside of an automotive headlamp using a 2D PIV method by Shiozawa et al. (2000) and Okada et al. (2002), but there has been no report on 3D velocity field measurements so far. The aim of this study is to obtain accurate 2D3C velocity fields to understand the complex velocity fields inside of actual automotive headlamps and to provide benchmark data for CFD validation. In order to accomplish the TR-SPIV measurement successfully, it is necessary to establish optical noise-elimination techniques to solve the refraction, reflection, and image-distortion problems caused by the complex shape of the lamp and the curvature of the lens surface. Careful calibration procedures and background optical noise removal method were developed and applied for the pre- and post-processing of TR-SPIV. Most CFD researches had assumed that the flow inside of automotive lamps is laminar, but the possibility of presence of turbulence has also claimed by previous works by Sousa et al. (2005) and Sokmen et al. (2014). In this study, an attempt to identify the presence of turbulence in the interior space of the headlamp was carried out. In addition, the effect of the light source such as a halogen bulb and an LED in the same headlamp case was also examined.

2 Experimental setup

Figure 1 shows a diagram of the SPIV experiment for measuring the internal flow in the headlamp. The selected headlamp model was from a Hyundai Grandeur IG vehicle, and internal flow measurements were conducted for a bulb-type and an LED-type headlamp.

The reasons to choose the specific headlamp model are as following. First, we need to choose the model which uses the light source of the low beam as both the halogen bulb type and the LED type in order to compare the difference of the flow according to the light source. Also, it is necessary to select a vehicle model with a little modification of the lamp interior structure when the light source can be changed. Lastly, we want to choose a headlamp model with many complain from customers about moisture problems. To meet all the above requirements, a Hyundai Grandeur IG model was selected.

The olive oil aerosol (diameter = 1 - 2 μm) that was used as PIV tracer particles was atomized by a Laskin nozzle and injected through a vent hole behind the headlamp. A laser sheet (Continuous Wave, 532 nm, 5W, LVI technology INC.) was generated using a cylindrical and spherical lens. To obtain stereo particle images, two high-speed cameras (Phantom VEO 410L) were placed at an angle of 15 degrees each at a vertical angle from the laser sheet. Because the laser plane and the high-speed camera sensor plane are not parallel to each other, we used a tilting lens (Nikon, 85 mm) to satisfy the Scheimpflug condition. A pulse generator (BNC 555 model) was used to input an external trigger to the cameras to acquire the particle image at the same time.

In the case of PIV measurement for headlamp, the particle images suffer from background noise by reflection. This background noise should be minimized because it causes errors in PIV analysis, and it must be removed in order to improve the accuracy of PIV measurement. So, we applied a POD-based background noise removal method developed by M. A. Mendez et al. [19]. From this post-processing procedure on the image noise removal, we could get the relatively clean particle image for the TR-SPIV analysis.

All particle images were acquired at a rate of 250 frames per second. Experiments were performed considering the exposure time in the camera software. The sampling rate is 250 fps, but the exposure time is set to 1 ms in consideration of particle motion. Therefore, there was no significant problem in cross-correlation analysis. During the experiment, the internal flow was observed after turning on the

low-beam lamp and the position-signal lamp. Each of the measurement planes was calibrated, and five grid images were acquired by moving the grid in 0.5-mm increments in the depth direction for calibration in one plane. Because of the complex geometry of the outer lens of the headlamps, a particle image can be severely distorted through an optical path. To compensate for distortion in an image, calibration was conducted using a detachable outer lens placed between the calibration target and cameras. The calibration target surface is located at the same plane as the laser light sheet.

Figure 2 shows the fields of view for the time-resolved SPIV measurement. View 1 and View 2 are side views that are parallel with the direction of light propagation. As shown in figure 2(a), View 1 is the central plane of the low-beam bulb, and the lighting is on all the time. View 2 is the central plane of the high-beam bulb, which is off during measurements. View 3 and View 4 are front views and are perpendicular to View 1 and View 2, respectively. As shown in figure 2(b), the laser light sheet is located at the middle of the cavity between the bulb and the outer lens. View 3 and View 4 are 43 mm from the bulb's center point at the low-beam bulb area and 36 mm from the center point of the high beam, as shown in figures 2(b) and (c). The X axis is in the light-projection direction, the Y axis is perpendicular to the light projection direction, and the Z axis is the opposite direction of gravity.

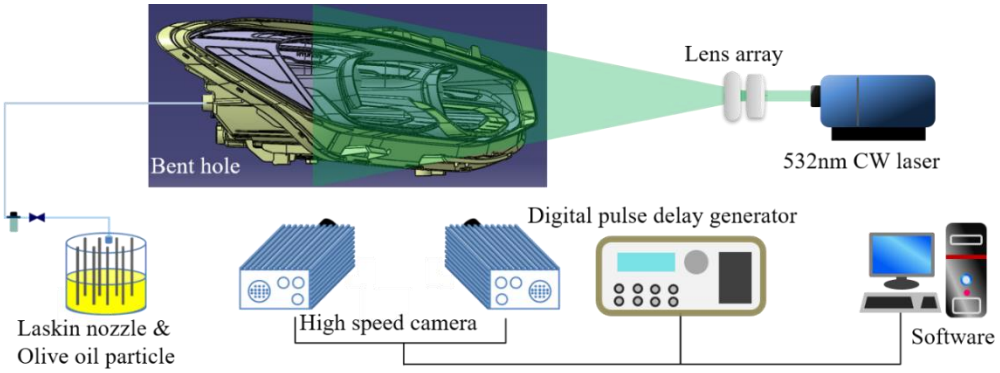

Figure 1: Diagram of time-resolved stereoscopic PIV setup

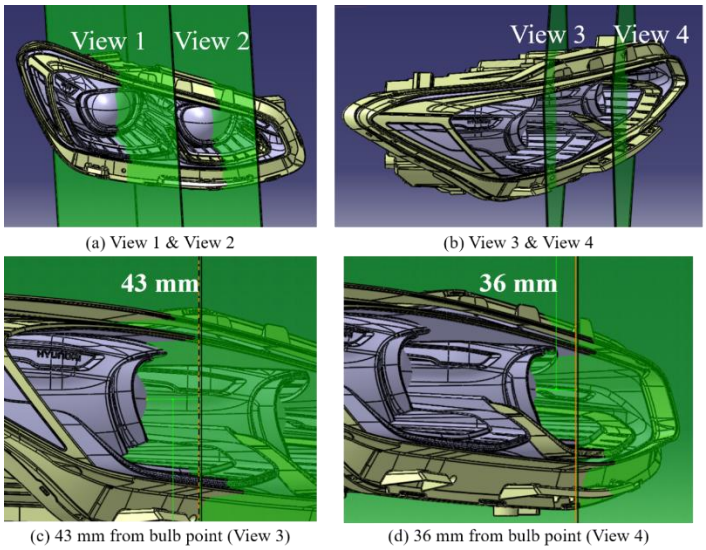

Figure 2: Fields of view for time-resolved SPIV measurement

3 Results and discussion

Figure 3 shows the ensemble-averaged 2D3C velocity fields at the View 1 plane obtained at 30, 60, and 90 minutes. The arrows represent the 2D in-plane velocity components, and the contours represent the out-of-plane velocity components. The red color represents the flow from the direction coming out of the plane, and blue color represents flow in the direction coming into the plane. A three-dimensional flow structure is clearly seen in this figure for both types of headlamps. However, some differences in the flow fields are observed between the bulb and LED types.

Figures 3(a), 3(b), and 3(c) show the ensemble-averaged 2D3C velocity fields in the bulb-type headlamp obtained at 30, 60, and 90 minutes from when the lighting turns on. The overall flow structures look the same, but the thermally driven natural convection becomes stronger as time goes on. The bulb-type headlamp generates a strong thermal plume on the bulb center because the surface temperature of the lens is heated up to 155°C by strong radiation. As a result, hot air rises in the vertical direction, and the plume impinges on the upper reflector. The plume that is horizontally bent by the reflector reaches the outer lens and then flows down along the lens-wall surface. The flow before steady state has a relatively low temperature on the surface of the bulb, so it cannot recirculate to the whole lens wall due to the insufficient momentum, as shown in figure 3 (a).

Figures 3(d), 3(e), and 3(f) illustrate the ensemble-averaged 2D3C velocity fields in the LED-type headlamp obtained at 30, 60, and 90 minutes from when the lighting turns on. The overall flow structures look the same, but the flow changes slightly as time goes on. In the case of the LED type, the maximum temperature is lower than that of the bulb type in steady state. Therefore, a strong thermal plume cannot be generated by the LED light source. Instead, a strong horizontal flow comes from behind the LED lens to the inside of the headlamp. This occurs because there is a high-temperature spot (around 250°C) at the LED heat dissipater located at the back of the light source. Therefore, the strong thermal plume being generated at the rear of the LED is bent through the narrow horizontal channel between the light source and the reflector. The flows in the View 1 plane of both types of headlamps look similar, but the flow generation mechanisms are different.

The remarkable difference between the two types in view 1 is the distribution of the flow by the reflector and the light source. The reasons for this difference are the temperature distribution at the light source, and the space between the light source and the reflector. The bulb type has a relatively narrow space, whereas the LED type has a wide space. The difference in geometry can change the flow pattern.

The most remarkable result of this measurement is that the velocity component in the direction perpendicular to the X-Z plane (side view) is larger than the velocity components in the measurement plane. Both the bulb and the LED types have incoming and outgoing flow at the end of the reflector because a strong vortex flow to the Y axis is generated. This result shows that a strong 3D flow is formed above the light source due to the complex internal structure of the headlamp.

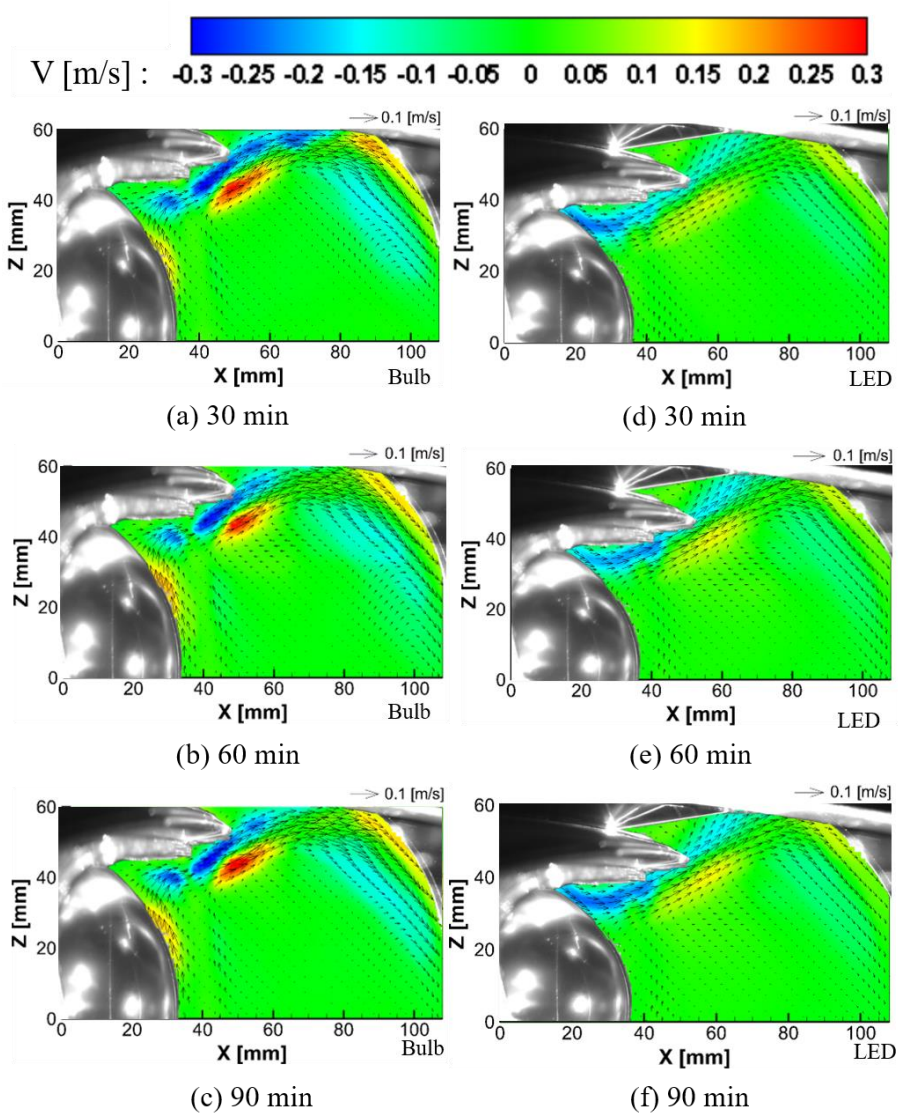

Figure 3: Spatial and temporal variations of 2D3C velocity fields at View 1 plane. Bulb type (a, b, c) and LED type (d, e, f)

Figure 4 shows the ensemble-averaged 2D3C velocity fields at the View 2 plane obtained at 30, 60, and 90 minutes from turning on the headlamp's low beam. The high-beam bulb and LED in this plane are turned off. In this side view, there is no strong natural convection or three-dimensional flows compared to the flows in View 1. Figures 4(a), 4(b), and 4(c) present the ensemble-averaged 2D3C velocity fields in the bulb-type headlamp obtained at 30, 60, and 90 minutes from turning on the headlamp's low beam. The overall flow patterns look the same, but slight changes with time can be seen. As observed in View 1, the out-of-plane velocity component is much bigger than the in-plane velocity components in View 2 as well. Incoming velocity occurs at the upper region of the high-beam bulb, and outgoing velocity occurs at the bottom side. There is also a large vortex with respect to the X axis. The flow seems stagnant in most of the plane, especially the central part.

Figures 4(d), 4(e), and 4(f) illustrate the ensemble-averaged 2D3C velocity fields in the LED-type headlamp obtained at 30, 60, and 90 minutes from the start of the experiment. The overall flow structures look the same, but the flow changes slightly as time goes on. The velocity field at steady

state looks two-dimensional, and a slow X-axis vortex is shown in figure 4(f). It is interesting to note that the flow characteristics in the bottom region of View 2 are significantly different between the bulb and LED headlamp. This means that the source region of the airflow is different in two types of headlamps, so the returning flow pattern after reaching the outer lens surface may vary. Despite the similarity of the internal space of the lamp, the flow pattern depending on the source of the flow turns out to be an important design parameter to consider to improve the flow and prevent condensation problems in automotive headlamps.

In View 2, the difference between the two types is the flow structure in the bottom region. This is because the circulation by the three-dimensional flow shows a better performance in the LED type.

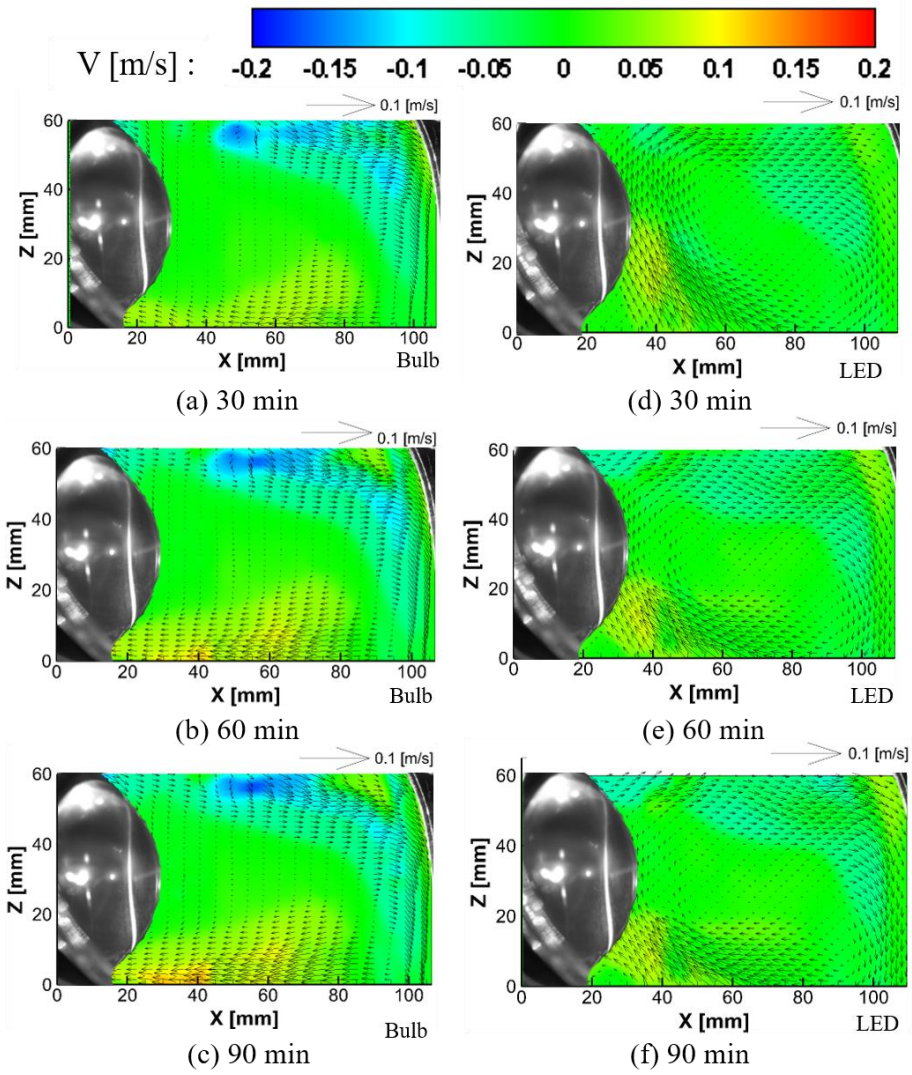

Figure 4: Spatial and temporal variations of 2D3C velocity fields at View 2 plane. Bulb type (a, b, c) and LED type (d, e, f)

Figure 5 shows the ensemble-averaged 2D3C velocity fields at the View 3 plane obtained at 30, 60, and 90 minutes from turning on the headlamp's low beam. For both the bulb and LED-type headlamps, the three-dimensional component does not appear in this front-view section. This occurs because the frontal measurement section passes through the region where the flow stagnates in the side view.

The detailed flow field in the View 3 plane is different between the bulb and LED-type headlamps. Figures 5(a), 5(b), and 5(c) show the ensemble-averaged 2D3C velocity fields in the bulb-type headlamp obtained at 30, 60, and 90 minutes from the start time. Changes in the flow field with time are not apparent. The flow near the outer lens is very low. Furthermore, there is no flow in the lower part of the outer lens of bulb-type headlamp. This situation leads to easy condensation at the inner wall of the lens due to the lack of convection.

Figures 5(d), 5(e), and 5(f) demonstrate the ensemble-averaged 2D3C velocity fields in the View 3 plane of the LED-type headlamp obtained at 30, 60, and 90 minutes from starting the experiment. The development of flow near the lens wall can be seen with time goes on. The velocity field at steady state looks two-dimensional. However, the fluid continues moving along the side wall of the lens, which increases the convective heat transfer and delays the condensation in the case of the LED-type headlamp.

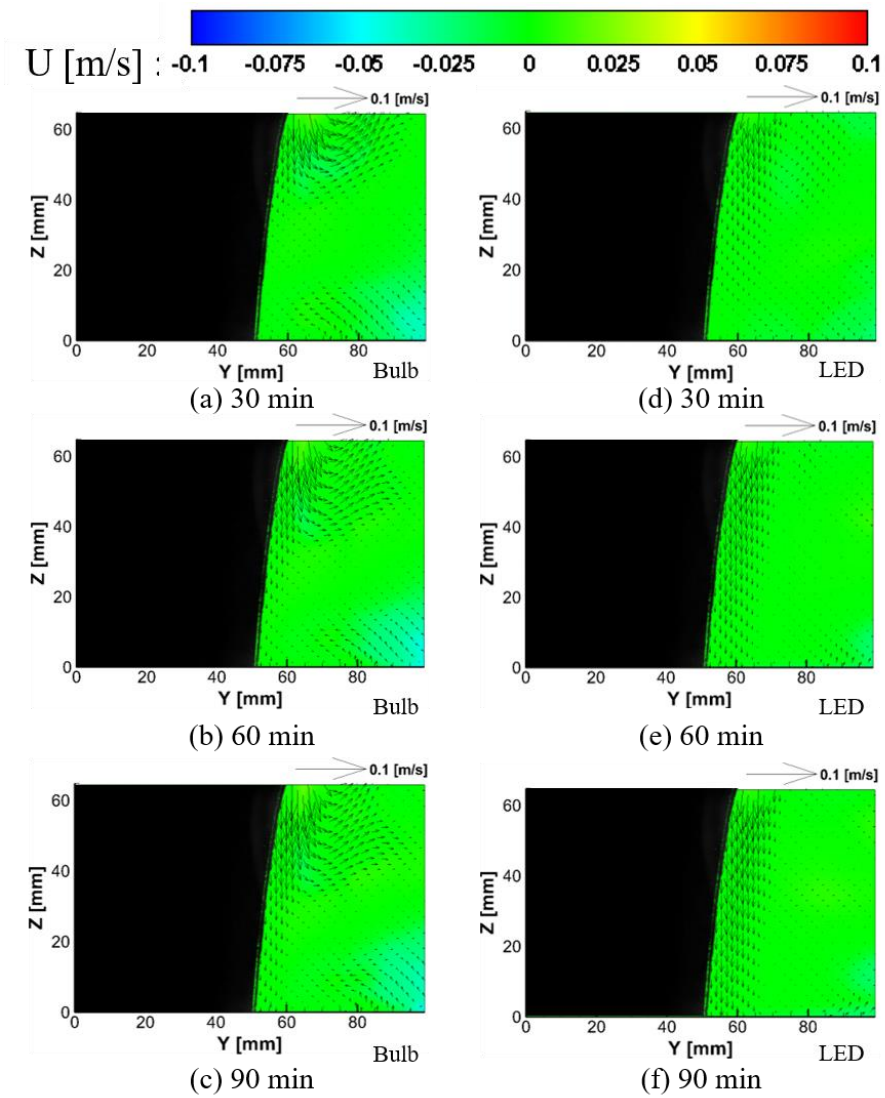

Figure 5: Spatial and temporal variations of 2D3C velocity fields at View 3 plane. Bulb type (a, b, c) and LED type (d, e, f)

Figure 6 shows the ensemble-averaged 2D3C velocity fields at the View 4 plane obtained at 30, 60, and 90 minutes from the start. This plane is the middle of the high-beam cavity. Since the high-beam lamp is off during the experiment, the temperature change with time is small. Therefore, a noticeable change is not observed in the flow field with time in View 4 for both types of headlamps. However, the flow pattern is different between the bulb and LED type, as shown in figures 6(c) and 6(f) at steady state. In the case of the bulb type, there are velocity vectors in the middle of View 4, but no such flows are observed in the LED-type headlamp.

The major difference between View 3 and View 4 is whether the flow is well transported to the bottom region of the outer lens. This difference can be explained by the temperature gradient. The bulb type cannot transport fluid in the bottom region of the outer lens according to the temperature gradient but extends in the Y direction. In the case of the LED, the flow is transported to the bottom region by the temperature gradient effect.

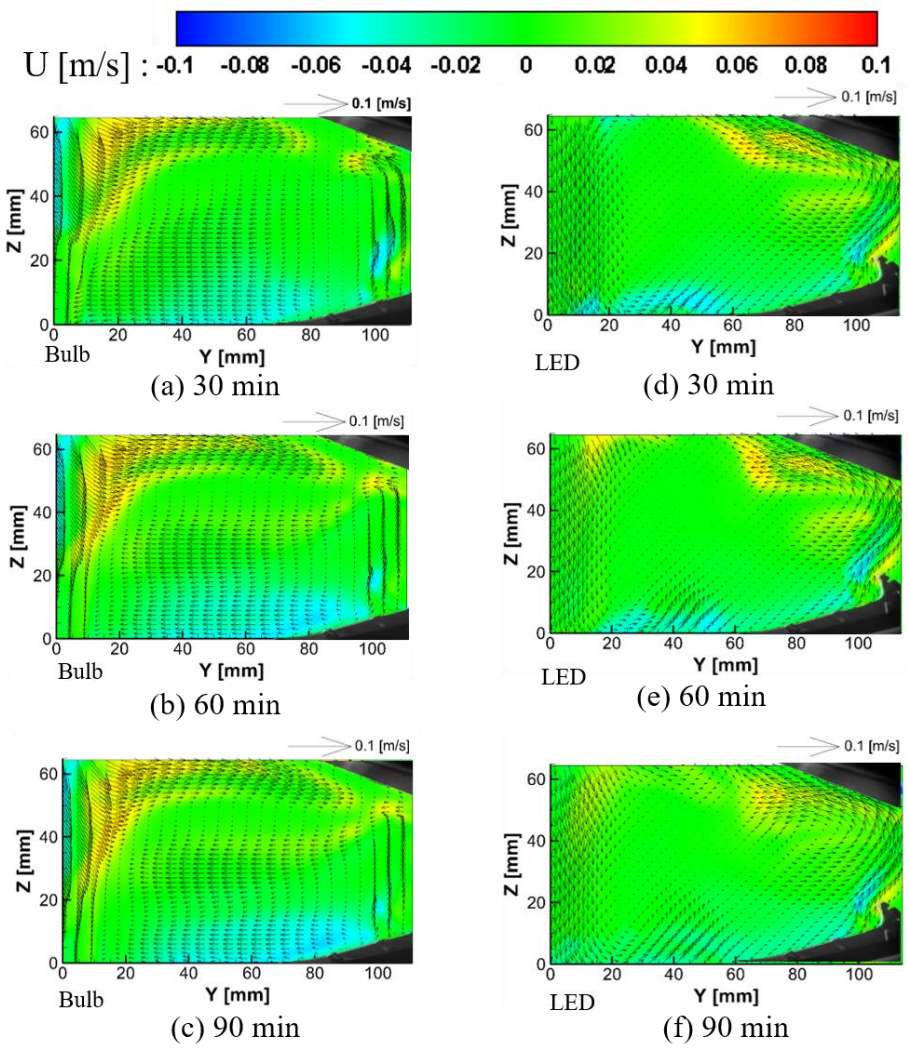

Figure 6: Spatial and temporal variations of 2D3C velocity fields at View 4 plane. Bulb type (a, b, c) and LED type (d, e, f).

4 Conclusion

In this study, the flow inside an automobile headlamp was quantitatively visualized by applying a time-resolved SPIV technique. The temporal variation of the inner surface temperature was measured for the bulb-type and the LED-type headlamps of a Hyundai Grandeur IG vehicle. It was found that the steady state was reached at 90 minutes after the lighting was turned on.

The TR-SPIV measurement showed that the flow inside the headlamp has a strong three-dimensional flow field, and two or more vortex components are formed in a direction perpendicular to the beam propagation plane (X-Z plane). In addition, the bulb and LED-type headlamps showed that the generation of natural convection is totally different. In the case of the bulb type, strong natural convection was generated on the surface of the high-temperature lens, and the thermal plume moved upward to the overall flow field. However, in the case of the LED type, the main flow was supplied to the inner space of the headlamp due to the natural convection generated in the heat sink behind the LED. The bulb type cannot transport fluid in the bottom region of the outer lens according to the temperature gradient but extends in the Y direction. In the case of the LED, the flow is well transported to the bottom region by the temperature gradient effect. The results imply that the bulb type headlamp has more possibility of condensation on the outer lens compared to the LED type headlamp. The bulb type headlamp generates turbulence locally due to intricate internal structures such as the reflector, and a thermal plume was strongly formed. However, most of the flow fields have the characteristics of laminar flow.

Acknowledgements

This study was supported by the National Research Foundation of Korea (NRF) funded by the Korean government (MSIT) (no. 2018R1A2B2007117).

References

Okada Y, Nouzawa T, and Nakamura T (2002) CFD analysis of the flow in an automotive headlamp. *JSAE review* 23:95

Shiozawa T, Nakanishi A, Ozawa T, Oki T, Tsuda N, Saga T, and Kobayashi T (2000) Thermal air flow analysis of an automotive headlamp-the PIV measurement and the CFD simulation by using a skeleton model. *SAE Technical Paper*

Sokmen KF, Pulat E, Yamankaradeniz N, and Coskun S (2014) Thermal computations of temperature distribution and bulb heat transfer in an automobile headlamp. *Heat and mass transfer* 50:199

Sousa JMM, Vogado J, Costa M, Bensler H, Freek C, and Heath D (2005) An experimental investigation of fluid flow and wall temperature distributions in an automotive headlight. *International Journal of Heat and Fluid Flow* 26:709